The Close Link of Pancreatic Iron With Glucose Metabolism and With Cardiac Complications in Thalassemia Major: A Large, Multicenter Observational Study

Diabetes Care 2020;43:2830–2839 | https://doi.org/10.2337/dc20-0908

Alessia Pepe,[1] Laura Pistoia,[1] Maria Rita Gamberini,[2] Liana Cuccia,[3] Angelo Peluso,[4] Giuseppe Messina,[5] Anna Spasiano,[6] Massimo Allò,[7] Maria Grazia Bisconte,[8] Maria Caterina Putti,[9] Tommaso Casini,[10] Nicola Dello Iacono,[11] Mauro Celli,[12] Angelantonio Vitucci,[13] Pietro Giuliano,[14] Giuseppe Peritore,[15] Stefania Renne,[16] Riccardo Righi,[17] Vincenzo Positano,[1] Vincenzo De Sanctis,[18] and Antonella Meloni[1]

OBJECTIVE

We systematically explored the link of pancreatic iron with glucose metabolism and with cardiac complications in a cohort of 1,079 patients with thalassemia major (TM) enrolled in the Extension-Myocardial Iron Overload in Thalassemia (E-MIOT) project.

RESEARCH DESIGN AND METHODS

MRI was used to quantify iron overload (T2* technique) and cardiac function (cine images) and to detect macroscopic myocardial fibrosis (late gadolinium enhancement technique). Glucose metabolism was assessed by the oral glucose tolerance test (OGTT).

RESULTS

Patients with normal glucose metabolism showed significantly higher global pancreas T2* values than patients with impaired fasting glucose, impaired glucose tolerance, and diabetes. A pancreas T2* <13.07 ms predicted an abnormal OGTT. A normal pancreas T2* value showed a 100% negative predictive value for disturbances of glucose metabolism and for cardiac iron. Patients with myocardial fibrosis showed significantly lower pancreas T2* values. Patients with cardiac complications had significantly lower pancreas T2* values. No patient with arrhythmias/heart failure had a normal global pancreas T2*.

CONCLUSIONS

Pancreatic iron is a powerful predictor not only for glucose metabolism but also for cardiac iron and complications, supporting the close link between pancreatic iron and heart disease and the need to intensify iron chelation therapy to prevent both alterations of glucose metabolism and cardiac iron accumulation.

Thalassemia major (TM) is a hereditary anemia characterized by ineffective erythropoiesis and hemolysis, requiring regular red blood cell transfusions to sustain life. A major drawback of this treatment is iron overload, which can cause organ dysfunction (1). The introduction of chelation therapy has improved the survival of TM patients, but cardiac complications remain the main cause of mortality, while endocrinopathies are the most frequent morbidities. Diabetes is the third-most-common endocrine complication (2). In a large cohort of well-treated and well-chelated TM patients, the

[1]Magnetic Resonance Imaging Unit, Fondazione G. Monasterio CNR-Regione Toscana, Pisa, Italy
[2]Dipartimento della Riproduzione e dell'Accrescimento, Day Hospital della Talassemia e delle Emoglobinopatie, Azienda Ospedaliero–Universitaria di Ferrara - Arcispedale Sant'Anna, Ferrara, Italy
[3]Unità Operativa Complessa Ematologia con Talassemia, Azienda di Rilievo Nazionale ed Alta Specializzazione Ospedali Civico Di Cristina Benfratelli, Palermo, Italy
[4]Struttura Semplice di Microcitemia, Ospedale "SS. Annunziata" ASL Taranto, Taranto, Italy
[5]Centro Microcitemie, Azienda Ospedaliera "Bianchi-Melacrino-Morelli," Reggio Calabria, Italy
[6]Unità Operativa Semplice Dipartimentale Malattie Rare del Globulo Rosso, Azienda Ospedaliera di Rilievo Nazionale "Antonio Cardarelli," Napoli, Italy
[7]Ematologia Microcitemia, Ospedale San Giovanni di Dio–Azienda Sanitaria Provinciale Crotone, Crotone, Italy
[8]Centro di Microcitemia, Unità Operativa Ematologia, Azienda Ospedaliera Cosenza, Cosenza, Italy
[9]Clinica di Emato-Oncologia Pediatrica, Dipartimento di Salute della Donna e del Bambino, Azienda Ospedaliero di Padova–Università di Padova, Padova, Italy
[10]Centro Talassemie ed Emoglobinopatie, Ospedale "Meyer," Firenze, Italy
[11]Centro Microcitemia, Day Hospital Thalassemia, Poliambulatorio "Giovanni Paolo II," Ospedale Casa Sollievo della Sofferenza IRCCS, San Giovanni Rotondo, Italy
[12]Unità Operativa Complessa di ImmunoEmatologia, Dipartimenti Assistenziali Integrati di Pediatria e Neuropsiachiatria Infantile, Roma, Italy
[13]Ematologia con Trapianto-Servizio Regionale Talassemie, Dipartimento dell'Emergenza e dei Trapianti d'Organo, Azienda Universitaria Ospedaliera Consorziale - Policlinico Bari, Bari, Italy
[14]Cardiologia con UTIC, Azienda di Rilievo Nazionale ad Alta Specializzazione Civico Di Cristina Benfratelli, Palermo, Italy

prevalence of diabetes was 9% (3), but its incidence can reach also 20–30%, depending on the age of assessment, the intensity of chelation, and the related patient compliance (4). Moreover, the increasing life expectancy will make diabetes a more significant clinical problem, due to the combination of iron-mediated toxicity and natural aging. It is known from pathological, epidemiological, and clinical studies that iron accumulates selectively within β-cells in TM patients and that impaired glucose tolerance (IGT) and its progression toward overt diabetes depend on the severity and duration of severe iron overload. However, the exact mechanisms of iron-induced diabetes are unclear, and it is likely mediated by different mechanisms, such as insulin deficiency, insulin resistance, hepatic dysfunction, and genetic factors (4,5).

The T2* MRI has emerged as the technique of choice for the noninvasive, sensitive, fast, and reproducible quantification of organ-specific iron overload (6,7). Despite extensive research about T2* quantitative MRI of hepatic and cardiac iron, there are still few reports on pancreatic iron and its clinical correlations. The correlation between pancreas T2* and altered glucose metabolism is not well defined. In a small cohort of 59 TM patients, Noetzli et al. (8) found a significant higher frequency of glucose dysregulation among patients with pancreatic iron overload versus patients without pancreatic iron overload (71.8% vs. 15.0%; $P < 0.0001$) and pancreas T2* emerged as the strongest overall predictor of glucose dysregulation. Conversely, other studies showed comparable pancreatic T2* values in patients with normal and impaired glucose metabolism (9–11).

Preliminary studies on small populations showed a correlation between pancreatic and cardiac T2* values (9–13), with a normal pancreas T2* value showing a negative predictive value of 100% for cardiac iron. A more profound link between pancreatic iron and heart disease could be expected based on data from a large historical cohort of TM patients demonstrating that diabetes increases the risk for heart failure (HF), hyperkinetic arrhythmias, and myocardial fibrosis independently by the levels of cardiac iron (3). To the best of our knowledge, no other studies have systematically investigated the link between the pancreas and cardiac diseases in TM.

The aim of this multicenter study was to systematically explore the link of pancreatic iron with glucose metabolism and with cardiac complications in a large cohort of well-treated TM patients enrolled at basal in the prospective Extension-Myocardial Iron Overload in Thalassemia (E-MIOT) project.

RESEARCH DESIGN AND METHODS

Study Population

We considered 1,079 β-TM patients (576 females and 503 males, mean age 37.79 ± 10.11 years, age range 7–65 years), consecutively enrolled at basal in the E-MIOT project from October 2015 to August 2019. The aim of the E-MIOT project was to explore prospectively at 18 and 36 months the link of pancreatic iron quantified by MRI with glucose metabolism and with cardiac complications in a large cohort of TM patients. E-MIOT is an Italian network constituted by 11 MRI sites and 66 thalassemia centers, where MRI exams are performed using homogeneous, standardized, and validated procedures for the heart, the liver, and the pancreas (14–16). All centers are linked by a shared database where all clinical, laboratory, and instrumental data are collected.

All patients were regularly transfused to maintain a pretransfusion hemoglobin concentration >9–10 g/dL, and MRI scanning was performed within 1 week before regular scheduled blood transfusion.

The study complied with the Declaration of Helsinki and was approved by the ethics committees of all the Italian MRI sites involved in the study (Ancona, Campobasso, Catania, Ferrara, Lamezia Terme, Napoli, Palermo, Pisa, Roma, and Taranto, Italy). All patients gave written informed consent.

MRI Protocol

All the patients underwent MRI using conventional clinical 1.5T scanners of three main vendors (GE Healthcare, Philips Healthcare, and Siemens Healthineers) equipped with eight-element phased-array receiver surface coil.

For iron overload assessment, T2* multiecho sequences were acquired. Five or more axial slices covering the whole abdomen and including the whole pancreas (17), a midtransverse hepatic slice (18), and three parallel short-axis views (basal, medium, and apical) of the left ventricle (LV) (14,19) were obtained. T2* image analysis was performed using custom-written, previously validated software (HIPPO MIOT) (20). Three small regions of interest were manually drawn over pancreatic head, body, and tail encompassing parenchymal tissue and with care taken to avoid large blood vessels or ducts and areas involved in susceptibility artifacts from gastric or colic intraluminal gas (21). Global pancreatic T2* value was calculated as the mean of T2* values from the three regions; 26 ms was previously demonstrated to be the lowest threshold of normal T2* pancreatic value (17). Hepatic T2* values were calculated in a circular ROI (22) and were converted into liver iron concentration (LIC) using the Wood calibration curve (23,24). The myocardial T2* distribution was mapped into a 16-segment LV model, according to the American Heart Association (AHA)/American College of Cardiology (ACC) model. The global heart T2* value was obtained by averaging of all segmental T2* values. A T2* measurement >20 ms was taken as a "conservative" normal value (20,25). The reproducibility of the methodology had been previously assessed for all organs (14–16).

Steady-state free procession cine images were acquired in sequential 8-mm short-axis slices from the atrioventricular ring to the apex for assessment of biventricular function parameters quantitatively

[15]Unità Operativa Complessa di Radiologia, Azienda di Rilievo Nazionale ad Alta Specializzazione Civico Di Cristina Benfratelli, Palermo, Italy
[16]Struttura Complessa di Cardioradiologia-UTIC, Presidio Ospedaliero "Giovanni Paolo II," Lamezia Terme, Italy
[17]Diagnostica per Immagini e Radiologia Interventistica, Ospedale del Delta, Lagosanto, Italy
[18]Pediatric and Adolescent Outpatient Clinic, Quisisana Hospital, Ferrara, Italy
Corresponding author: Alessia Pepe, alessia.pepe@ftgm.it
Received 22 April 2020 and accepted 8 August 2020

in a standard way (26). The intercenter variability had been previously reported (27).

Per protocol, for detection of the presence of macroscopic myocardial fibrosis, standard late gadolinium enhancement technique was applied (28,29) with use of gadobutrol (0.2 mmoL/kg) in patients with age >10 years, a glomerular filtration rate >30 mL/min per 1.73 m^2, and at least one indication for the contrast medium administration based on the AHA consensus statement (past or current cardiovascular risk factors, hepatitis C virus [HCV] infection, myocardial iron overload (MIO), heart dysfunction, or cardiovascular disease) (30).

Assessment of Glucose Metabolism

For assessment of the disturbances of glucose metabolism, patients not already diagnosed with diabetes had an oral glucose tolerance test (OGTT) within 3 months from the MRI study at the reference thalassemia center.

All patients were required to fast overnight (at least 12 h). Baseline blood assessments of glucose and insulin were performed. Patients were given 1.75 g/kg (maximum dose of 75 g) glucose solution, and glucose and insulin were measured at 60 and 120 min. In the patients without known diabetes, we used the HOMA of insulin resistance (HOMA-IR) index to assess insulin resistance, and it was calculated as the product of fasting glucose and insulin levels divided by 22.5 (31). The HOMA of β-cell function (HOMA-B) index was used as a measure of β-cell function, and it was computed as the product of 360 and fasting insulin levels divided by the value of fasting glucose concentrations minus 63 (32).

Diagnostic Criteria

A fasting plasma glucose (FPG) <100 mg/dL and 2-h glucose <140 mg/dL were considered indicative of normal glucose tolerance. Impaired fasting glucose (IFG) was diagnosed in the presence of FPG levels between 100 and 126 mg/dL. IGT was defined as 2-h plasma glucose between 140 and 200 mg/dL, with an FPG <126 mg/dL. Diabetes was defined as FPG ≥126 mg/dL or 2-h plasma glucose ≥200 mg/dL during an OGTT or a random plasma glucose ≥200 mg/dL with classic symptoms of hyperglycemia or hyperglycemic crisis (33).

HF was diagnosed by clinicians based on symptoms, signs, and instrumental findings according to the AHA/ACC guidelines (34). Arrhythmias were diagnosed only if electrocardiogram documented and requiring specific medication. Arrhythmias were classified according to the AHA/ACC guidelines (35). Pulmonary hypertension was diagnosed if the transtricuspidal velocity jet was >3.2 m/s (36). The term "cardiac complications" included HF, arrhythmias, and pulmonary hypertension clinically active at the time of the MRI.

Statistical Analysis

All data were analyzed using SPSS, version 13.0. Continuous variables were described as mean ± SD, and categorical variables were expressed as frequencies and percentages.

For continuous values with normal distribution, comparisons between groups were made by independent-samples *t* test (for two groups) or one-way ANOVA (for more than two groups). Wilcoxon signed rank test or Kruskal-Wallis test was applied for continuous values with nonnormal distribution. Bonferroni post hoc test was used for multiple comparisons between pairs of groups.

Correlation analysis was performed by Spearman test. For determination of the best glucose and pancreas T2* cutoffs for discriminating the presence of an altered OGTT, the maximum sum of sensitivity and specificity was calculated from receiver operating characteristic (ROC) curve analysis.

In all tests, a two-tailed probability value of 0.05 was considered statistically significant.

Data and Resource Availability

The data that support the findings of this study are available from https://emiot.ftgm.it/, but restrictions apply to the availability of these data, which were used under license for the current study and therefore are not publicly available. Data are, however, available from the authors upon reasonable request and with permission of A.Pep. No applicable resources were generated or analyzed during the current study.

RESULTS

Patients' Characteristics and Clinical Correlates

The mean global pancreatic T2* value was 12.12 ± 9.87 ms, and 958 patients (88.8%) had a pathological global pancreas T2*. The youngest patient included in the study (7 years old) showed a pathological global pancreas T2*.

Global pancreas T2* values were comparable between males and females (12.49 ± 9.70 ms vs. 11.79 ± 10.00 ms, respectively; $P = 0.243$), while patients with pathological global pancreas T2* were significantly older (38.64 ± 9.76 years vs. 31.08 ± 10.31 years; $P < 0.0001$).

Splenectomized patients (56.4%) showed significantly lower global pancreas T2* than patients with the spleen (10.63 ± 8.27 ms vs. 13.98 ± 11.46 ms; $P < 0.0001$).

Pancreatic Iron and Glucose Metabolism

One hundred and twenty-nine patients (11.9%) were already diagnosed with diabetes, and 779 were tested for blood glucose. Of the patients, 15.8% (170) did not follow the current position statements that recommend an OGTT annually after 10 years in TM patients (37,38). Seven percent of patients showed IFG, 11.8% IGT, and 17.5% diabetes, for a total of 36.3% with altered glucose metabolism. At ROC curve analysis, an FPG >98 mg/dL predicted the presence of an abnormal OGTT with a sensitivity of 60.4% and a specificity of 95.9% ($P < 0.0001$). The area under the curve was 0.83 (95% CI 0.80–0.86).

Table 1 shows the association of pancreatic T2* values and MRI LIC values with glucose and insulin levels evaluated during the OGTT. In patients without a history of diabetes, global pancreatic T2* values were inversely correlated with fasting, 1-h, and 2-h glucose levels and MRI LIC values were positively associated with fasting and 1-h glucose levels and inversely correlated with 2-h insulin levels. No association was found between pancreatic or hepatic iron and HOMA-IR index, while the HOMA-B index showed a weak positive association with pancreatic T2* values and a weak negative correlation with MRI LIC values. In patients diagnosed with diabetes based on the OGTT, no correlation was found between pancreatic or hepatic iron and glucose/insulin levels.

The 82.9% of the patients with a normal glucose metabolism had a pathological global pancreas T2* value.

Patients with normal glucose metabolism showed significantly higher global

Table 1—Association of pancreas T2* values and MRI LIC values with glucose and insulin concentrations

Variable	Mean ± SD	Correlation with global pancreas T2* values		Correlation with MRI LIC values	
		R	*P*	*R*	*P*
All patients with OGTT					
FPG (mg/dL)	89.03 ± 10.80	−0.237	<0.0001	0.090	0.019
1-h plasma glucose after OGTT (mg/dL)	139.29 ± 40.68	−0.213	<0.0001	0.126	0.007
2-h plasma glucose after OGTT (mg/dL)	118.69 ± 32.53	−0.229	<0.0001	0.019	0.673
Fasting plasma insulin (μU/mL)	8.30 ± 7.68	0.067	0.123	−0.071	0.102
1-h plasma insulin after OGTT (μU/mL)	49.47 ± 35.34	−0.054	0.566	−0.151	0.110
2-h plasma insulin after OGTT (μU/mL)	39.27 ± 34.83	−0.069	0.469	−0.270	0.004
HOMA-IR index	1.82 ± 1.66	0.027	0.538	−0.005	0.205
HOMA-B index (%)	166.79 ± 405.61	0.195	<0.0001	−0.135	0.002
Patients without diabetes					
FPG (mg/dL)	88.69 ± 10.40	−0.227	<0.0001	0.095	0.014
1-h plasma glucose after OGTT (mg/dL)	137.52 ± 38.89	−0.202	<0.0001	0.125	0.009
2-h plasma glucose after OGTT (mg/dL)	116.19 ± 27.39	−0.208	<0.0001	0.006	0.905
Fasting plasma insulin (μU/mL)	8.29 ± 7.63	0.082	0.060	−0.068	0.122
1-h plasma insulin after OGTT (μU/mL)	49.49 ± 35.94	−0.051	0.594	−0.146	0.128
2-h plasma insulin after OGTT (μU/mL)	38.62 ± 34.95	−0.048	0.620	−0.267	0.005
HOMA-IR index	1.82 ± 1.64	0.035	0.430	−0.053	0.231
HOMA-B index (%)	168.39 ± 409.50	0.192	<0.0001	−0.133	0.002
Patients with newly diagnosed diabetes (on the basis of OGGT)					
FPG (mg/dL)	104.20 ± 16.68	−0.036	0.899	−0.368	0.177
1-h plasma glucose after OGTT (mg/dL)	203.50 ± 52.81	0.420	0.175	−0.399	0.199
2-h plasma glucose after OGTT (mg/dL)	209.69 ± 63.23	−0.017	0.957	0.383	0.197
Fasting plasma insulin (μU/mL)	8.79 ± 70.22	−0.291	0.385	−0.227	0.502
1-h plasma insulin after OGTT (μU/mL)	48.63 ± 11.57	0.200	0.800	−0.400	0.600
2-h plasma insulin after OGTT (μU/mL)	57.03 ± 30.03	−0.786	0.214	−0.800	0.200
HOMA-IR index	2.14 ± 2.49	−0.333	0.318	−0.305	0.361
HOMA-B index (%)	91.59 ± 105.16	−0.209	0.537	−0.127	0.709

pancreas T2* values than patients with IFG (14.31 ± 11.31 ms vs. 8.82 ± 6.23 ms, respectively; $P < 0.0001$), IGT (14.31 ± 11.31 ms vs. 8.25 ± 5.03 ms; $P < 0.0001$), and diabetes (14.31 ± 11.31 ms vs. 7.87 ± 4.45 ms; $P < 0.0001$) (Fig. 1*A*). None of the patients without pancreatic iron overload had an abnormal OGTT. A normal global pancreas T2* value showed a negative predictive value of 100% for disturbances of glucose metabolism.

At ROC curve analysis, a global pancreas T2* <13.07 predicted the presence of an abnormal OGTT with a sensitivity of 86.9% and a specificity of 39.5% ($P < 0.0001$). The area under the curve was 0.65 (95% CI 0.62–0.68).

Pancreatic Iron and HCV Infection

On the basis of the presence of HCV antibodies and HCV RNA, a categorization in three groups was performed: patients negative (group 0) (37.1%), patients who eradicated the virus spontaneously or after treatment with antiviral therapy (group 1) (52.5%), and patients with chronic HCV infection (group 2) (1.4%). Patients in group 0 showed significantly higher global pancreas T2* values than patients in group 1 (15.21 ± 11.65 ms vs. 10.68 ± 8.82, respectively; $P < 0.0001$) and in group 2 (15.21 ± 11.65 ms vs. 9.36 ± 7.78; $P < 0.0001$). Compared with group 1 and group 2, group 0 showed a significant lower frequency of diabetes (7.5% vs. 22.6% and 7.5% vs. 24.1%; $P < 0.0001$ for both comparisons).

Eighty-four patients had at least one cardiac complication. Patients in group 0 showed a significant lower frequency of cardiac complications than patients in group 1 (4.6% vs. 11.7%; $P = 0.001$) and group 2 (4.6% vs. 12.8% $P = 0.006$).

Pancreatic Iron and Serum Ferritin Levels

Mean serum ferritin levels in the last 12 months were 1,058.42 ± 1,359.16 ng/mL. A weak inverse correlation was detected between global pancreas T2* values and mean serum ferritin levels ($R = -0.200$; $P < 0.0001$).

At ROC curve analysis, a serum ferritin level >630 ng/mL predicted the presence of pancreatic iron overload with a sensitivity of 51.9% and a specificity of 59.6% ($P = 0.031$). The area under the curve was 0.57 (95% CI 0.53–0.59).

Pancreas T2* and MRI Correlates

Mean MRI LIC values were 6.19 ± 9.25 mg/g dry wt. A significant inverse correlation was found between MRI LIC and pancreatic T2* values ($R = -0.331$; $P < 0.0001$).

Mean global heart T2* value was 36.88 ± 9.72 ms. Global pancreas T2* values showed a significant positive correlation with global heart T2* values ($R = 0.323$; $P < 0.0001$) and a significant negative correlation with the number of segments with pathological T2* ($R = -0.322$; $P < 0.0001$). No patients without pancreatic iron overload had significant cardiac iron overload. A normal global pancreas T2* value showed a negative predictive value of 100% for cardiac iron. Four groups of patients were identified by the cardiac segmental approach: 830 patients

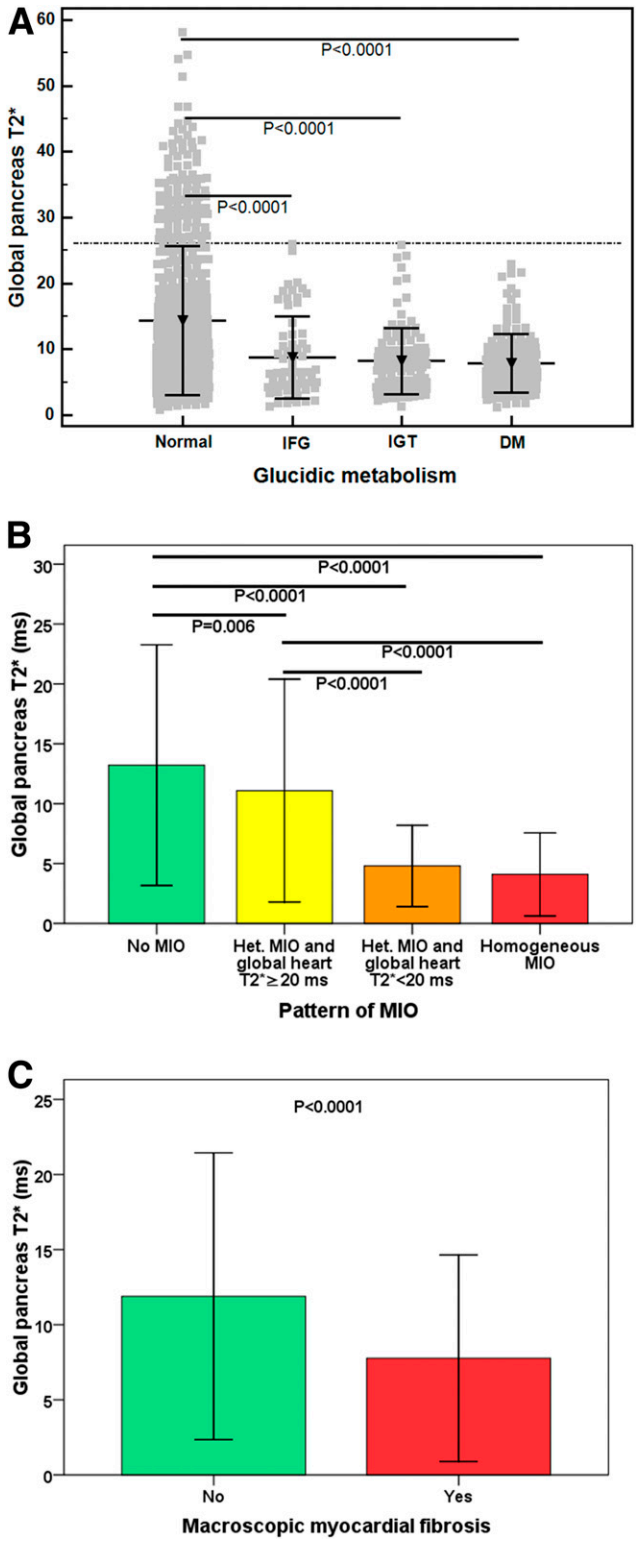

Figure 1—*A*: Global pancreas T2* values in the four groups of patients identified on the basis of the OGTT. The horizontal dotted line represents the cutoff for global pancreas T2* values. *B*: Global pancreas T2* values in the four groups of patients with different patterns of myocardial iron overload. Het., heterogeneous. *C*: Global pancreas T2* values in patients without and with myocardial fibrosis. DM, diabetes mellitus.

(77.0%) showed no MIO (all segments with T2* ≥20 ms), 152 patients (14.1%) showed an heterogeneous iron distribution (some segments with T2* ≥20 ms and others with T2* <20 ms) with global heart T2* ≥20 ms, 38 patients (3.5%) showed a heterogeneous MIO with global heart T2* <20 ms, and 58 patients (5.4%) showed a homogeneous MIO (all segments with T2* <20 ms). The global pancreas T2* was significantly higher in patients with no MIO than in the other three groups and in patients with heterogeneous MIO and global heart T2* ≥20 ms than in patients with heterogeneous MIO and global heart T2* <20 ms and patients with homogeneous MIO (Fig. 1*B*).

Mean LV and right ventricular ejection fractions were, respectively, 62.62 ± 6.83% and 61.23 ± 7.12%, and no correlation with global pancreatic T2* values was detected.

Based on the AHA consensus statement (30), 964 patients had a clinical indication to evaluate myocardial fibrosis, but 620 refused the contrast medium administration. Macroscopic myocardial fibrosis was detected in the 28.8% of the 344 patients in whom the contrast medium was administered. Patients with myocardial fibrosis were significantly older (40.52 ± 9.93 years vs. 37.75 ± 9.20 years; $P = 0.004$) and showed significant lower global pancreas T2* values (7.77 ± 6.87 ms vs. 11.89 ± 9.55 ms; $P < 0.0001$) (Fig. 1*C*).

Pancreatic Iron and Cardiac Complications

Patients with cardiac complications ($N = 84$) showed significantly lower global pancreas T2* values (8.22 ± 5.23 ms vs. 12.55 ± 10.16 ms; $P = 0.001$).

Arrhythmias were found in 50 patients. The supraventricular arrhythmias (atrial fibrillation and atrial flutter) were the most common type (88.0%). Five patients (10.0%) had ventricular arrhythmias, while one (2.0%) showed a hypokinetic arrhythmia. Patients with arrhythmias had significantly lower global pancreas T2* values (7.78 ± 3.98 ms vs. 12.41 ± 10.16 ms; $P = 0.009$), and no patients with arrhythmias had a normal global pancreas T2* (Fig. 2*A*).

Twenty-five patients had HF. Patients with HF had significantly lower global pancreas T2* values (7.39 ± 3.65 ms vs. 12.34 ± 10.09 ms; $P = 0.015$), and no patients with HF had a normal global pancreas T2* (Fig. 2*B*).

Pancreatic Iron and Chelation Therapy

TM patients who had been receiving the same chelation therapy for >1 year were retrospectively selected. Five groups of

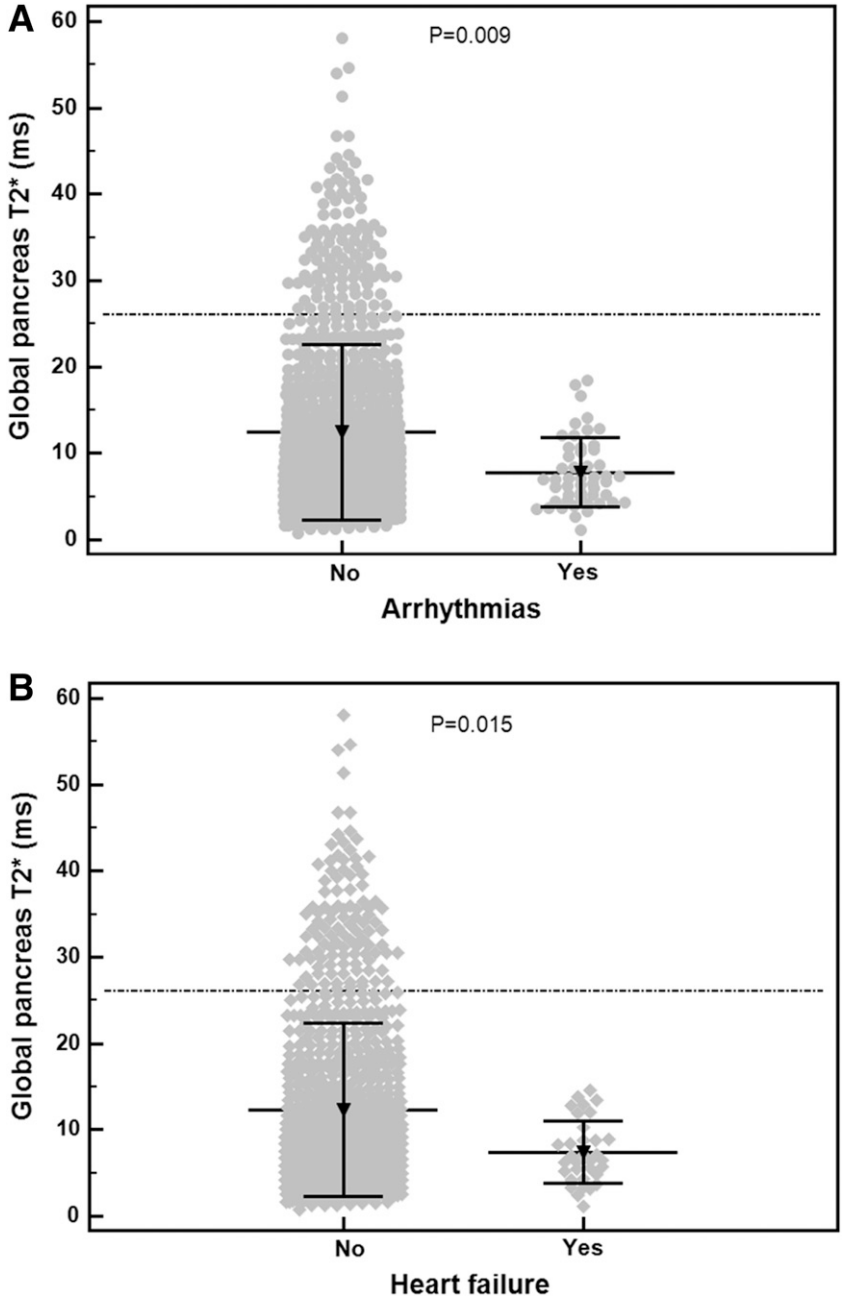

Figure 2—*A*: Global pancreas T2* values in patients without and with active arrhythmias. The horizontal dotted line represents the lower limit of normal for global pancreas T2* values. *B*: Global pancreas T2* values in patients without and with active HF. The horizontal dotted line represents the cutoff for global pancreas T2* values.

patients were identified: 96 patients treated with desferrioxamine (DFO), 161 with deferiprone (DFP), 326 with deferasirox (DFX), 71 with combined DFO+DFP, and 22 treated with sequential DFO/DFP.

The mean administered dosages of the chelators were as follows: *1*) DFP in combined regimen 81.46 ± 12.11 mg/kg body wt/day with a frequency of 6.79 ± 0.81 days/week and DFO in combined regimen 38.38 ± 8.48 mg/kg body wt/day with a frequency of 3.48 ± 1.53 days/week; *2*) DFO in monotherapy 37.39 ± 9.13 mg/kg body wt via subcutaneous route on 5.58 ± 0.89 days/week; *3*) DFP in monotherapy 81.36 ± 15.63 mg/kg body wt with a frequency of 6.96 ± 0.36 days/week; *4*) DFX 26.04 ± 7.69 mg/kg body wt and 21.08 ± 6.32 mg/kg body wt for the dispersible tablets and the film-coated tablet formulation, respectively, with a frequency of 7 days/week; *5*) DFP in sequential regimen 76.05 ± 16.09 mg/kg body wt/day with a frequency of 4.00 ± 0.79 days/week and DFO in sequential regimen 38.15 ± 5.52 mg/kg body wt/day with a frequency of 3.00 ± 0.56 days/week.

Table 2 shows the comparison between the combined group and the other treatment groups. Frequency of patients with a good/excellent compliance (correspondence between taken and prescribed chelator ≥60%) was significantly lower in the combined DFO+DFP group versus the three monotherapy groups. Patients in DFO+DFP therapy showed significantly lower global pancreas T2* values than all the other groups; significantly lower global heart T2* values than the DFP, DFX, and sequential DFO/DFP groups; significantly higher MRI LIC values than the DFO, DFX, and sequential DFO/DFP groups; and a significantly higher frequency of abnormal glucose metabolism than the DFX and sequential DFO/DFP groups.

All patients were naïve to pancreatic T2* MRI, while the majority of them had already had at least one MRI scan for the assessment of cardiac and hepatic iron levels. The frequency of patients with significant MIO (global heart T2* <20 ms) in the previous MRI was significantly higher in the DFO+DFP group versus all the other groups, and the frequency of patients with hepatic iron overload (MRI LIC >3 mg/g dry wt) in the previous MRI was significantly higher in the DFO+DFP group versus the DFO and DFX groups.

CONCLUSIONS

We evaluated pancreatic T2* values in the largest cohort ever reported of well-treated and well-chelated TM patients. Of our patients, 88.8% had a pathological global pancreas T2*, and this impressive prevalence is consistent with prevalence in previously published studies (12).

To our knowledge, this is the first study showing pancreatic iron accumulation as a time-dependent process starting in early childhood. Preliminary studies did not find a significant correlation between age and pancreatic T2*, probably due to significantly smaller and younger study cohorts (10,11).

Using a quantitative T2* technique, we demonstrated a higher pancreatic siderosis in splenectomized TM patients, in

Table 2—Intertreatment comparisons (combined versus the other chelation regimens) for patients receiving the same regimen for >1 year

	DFO+DFP group	DFO group	$P_{DFO+DFP}$ vs. DFO	DFP group	$P_{DFO+DFP}$ vs. DFP	DFX group	$P_{DFO+DFP}$ vs. DFX	Sequential DFO/DFP group	$P_{DFO+DFP}$ vs. sequential DFP/DFP
N	71	96		161		326		22	
Good/optimal compliance, %	82.9	96.8	0.005	92.5	0.029	94.4	0.001	95.5	0.178
Global pancreas T2* (ms)	8.17 ± 7.19	9.23 ± 6.65	0.019	11.01 ± 8.45	0.001	15.00 ± 11.41	<0.0001	11.52 ± 8.59	0.017
Global heart T2* (ms)	31.52 ± 14.26	34.65 ± 8.75	0.828	39.43 ± 6.35	0.002	38.08 ± 9.53	0.001	41.41 ± 5.23	0.005
MRI LIC values (mg/g dry wt)	7.89 ± 12.16	3.46 ± 4.53	<0.0001	6.54 ± 7.82	0.756	5.19 ± 7.52	0.016	2.48 ± 1.922	0.001
Patients with an abnormal OGTT	33 of 63 (52.4)	46 of 90 (51.1)	0.877	74 of 154 (48.1)	0.563	77 of 310 (24.8)	<0.0001	3 of 19 (15.8)	0.007
Patients with a previous MRI	63 (88.7)	86 (89.6)	0.861	138 (85.7)	0.534	257 (78.8)	0.056	19 (86.4)	0.718
Patients with hepatic iron overload at a previous MRI	40 of 63 (63.5)	30 of 86 (34.9)	0.001	79 of 138 (57.2)	0.403	116 of 257 (45.1)	0.009	8 of 19 (42.1)	0.097
Patients with myocardial iron overload at a previous MRI	20 of 63 (31.7)	9 of 86 (10.5)	0.002	7 of 138 (5.1)	<0.0001	15 of 257 (5.8)	<0.0001	1 of 19 (5.3)	0.033

Data are mean ± SD or *n* (%) unless otherwise indicated.

agreement with the only study by Matter, Allam, and Sadony (39), who explored this issue by a semiquantitative approach (the reduced signal intensity ratio as index of iron load). Since the spleen acts as a store for nontoxic iron, it protects the rest of the body from this iron (40).

Of patients, 36.3% showed altered glucose metabolism. Unfortunately, although Italy is recognized as a country with a universal and high-quality health national system, a consistent percentage of patients did not follow the current clinical recommendations about performing an OGTT annually after 10 years of age (37). We found that a fasting glucose >98 mg/dL identified an abnormal OGTT result. This cutoff is similar to that previously identified (97 mg/dL) by Noetzli et al. (8) in a small cohort of patients, and confirmation of the value would suggest the need to use lower cutoffs than population norms to increase specificity of the diagnosis in TM. Both impaired insulin release and insulin sensitivity contribute to abnormal glucose homeostasis in TM. The insulin deficiency is caused by iron deposition in the pancreatic cells (41), while insulin resistance can be due to hepatic iron deposition interfering with insulin's ability to suppress hepatic glucose production and iron deposition in the muscle decreasing glucose uptake (42). So, it is not surprising that in our cohort the HOMA-IR, the insulin resistance index, was not correlated with pancreatic T2* values. Moreover, in TM, insulin sensitivity was shown to be impaired also in apparently normoglycemic cases (43), and the truly increased insulin resistance may be masked by the use of indices based on fasting glucose and insulin concentrations. We detected a weak inverse correlation between HOMA-B, reflecting the fasting β-cell function, and increased iron deposition in the pancreas and in the liver. However, the correlation of hepatic iron with glycemic metabolic parameters is inferior to that of pancreatic iron, highlighting the importance of quantifying iron directly in the pancreas. Patients with normal glucose metabolism showed significantly higher global pancreas T2* values than patients with IFG, IGT, and diabetes, and a normal global pancreas T2* value showed a negative predictive value of 100% for disturbances of glucose metabolism. However, the 82.9% of the patients with a normal glucose metabolism had a pathological global pancreas, indicating the low specificity of pancreatic iron for the glucose dysregulation and supporting the hypothesis of a latency time before pancreatic iron could cause IGT and overt diabetes. We introduced a pancreatic T2* cutoff value of 13 ms for prediction of abnormal glucose metabolism and, despite poor specificity (~40%), this value may help to identify the patients at high risk for glucose dysregulation. In these patients, it would be prudent to escalate or modify the iron chelation therapy to prospectively prevent glucose dysregulation. Unlike cardiac dysfunction, β-cell damage is not 100% reversible. The prevalence of diabetes in the current study cohort was 17.5%, significantly higher than that detected in a previous cohort of Italian patients (9.0%; $P < 0.0001$), homogeneous for treatment but significantly younger. This datum is a consequence of the increased longevity of the TM population.

Our study confirms the role of the HCV infection in the development of diabetes (3,28,44). No data are available in

literature about the association between HCV infection and higher levels of iron deposition in the pancreas. HCV reduces the levels of hepcidin, resulting in elevated iron absorbed by duodenal enterocytes and release of iron from the liver and the reticuloendothelial system (45). Of note, it has been shown that also pancreatic β-cells express hepcidin (46) and that HCV can be present in human pancreatic β-cells (47). Importantly, a significant association was found between HCV infection and cardiac complications, strengthening the need to analyze HCV as a systemic disease in which extrahepatic consequences increase the weight of its pathological burden.

The significant negative correlation between serum ferritin levels and pancreatic iron overload confirms the findings from other studies (11,48); however, the correlation and the ROC curve are too weak for estimation of pancreatic iron by serum ferritin levels in clinical practice.

In agreement with previous studies on a small study population, we found a significant correlation between hepatic and pancreatic iron overload (10,11,49).

Moreover, in this large population we confirmed the association between cardiac and pancreatic hemosiderosis by a myocardial segmental analysis and the 100% negative predictive value of a normal global pancreas T2* value for cardiac iron (11,12), probably due to the same L-type calcium iron channels in the two organs. As a consequence, it is strongly recommended to incorporate in clinical practice T2* pancreatic measurements as prospective markers of cardiac iron risk. Moreover, performing abdominal MRI could significantly reduce need of sedation in young patients, costs, and magnet time, particularly in countries where it is difficult to perform cardiac MRI.

We were not able to show an association between LV ejection fraction and pancreatic T2* values confirming that cardiac dysfunction in TM patients is not related only to iron (27,29).

We showed for the first time an association between pancreatic iron and macroscopic myocardial fibrosis. As demonstrated also in this study, HCV infection is related to a higher risk of iron in the pancreas and consequently of diabetes in TM population. In a large retrospective historical TM cohort, diabetes was associated with a significant higher risk of myocardial fibrosis and cardiac complications, HF, and hyperkinetic arrhythmias (3). On the other hand, in TM, HCV infection is one of the possible mechanisms for macroscopic myocardial fibrosis through both myocarditis directly (28,50) and pancreas and liver damage with the development of diabetes indirectly (3,51). This physiopathologic link well supports how the pancreatic iron burden was strongly associated with the presence of myocardial fibrosis and cardiac complications and how all patients with HF and arrhythmias had a pathologic global pancreas T2* value. On the other hand, prospective data have demonstrated myocardial fibrosis as the strongest MRI predictor for HF and cardiac complications in TM (29), and the high percentage of patients who refused the administration of contrast medium to detect myocardial fibrosis against the current recommendation is worrying (30). The presence of many patients without cardiac complications but with pancreatic could be due to the fact that pancreatic iron deposition is an early event. A prolonged pancreatic iron exposition can cause both overt diabetes and cardiac iron overload, increasing the risk for development of cardiac complications. Longitudinal prospective studies could be useful to better clarify the temporal association between pancreatic iron and pancreatic dysfunction and cardiac iron.

Our analysis on the subgroup of patients treated with the same chelation regimen for a minimum of 12 months revealed higher levels of pancreatic, cardiac, and hepatic iron in patients treated with a mild combined DFO+DFP therapy. Most of our patients were not naïve to T2* MRI in heart and liver, and the patients in the combined group were those who had showed at the previous MRI the most severe iron burden in these two organs. So, our findings probably simply reflect the current clinical practice about the more frequent use of combined DFP+DFO therapy in heavily iron-loaded patients. It seems extremely hard to remove iron from the pancreas, and well-designed, prospective studies are clearly necessary to detect the most effective chelation regimen in removing pancreatic iron.

Limitations

This study suffers from some limitations. *1*) We do not have information on iron burden, usually estimated through the transfusional iron intake. The availability of such data would help evaluate the generalizability of the findings to other forms of thalassemia as well as aplastic anemias. However, we are planning to include this information in future studies. And *2*) since no blood samples were obtained 30 min after the load during the OGTT, we could not measure the insulinogenic index as a marker of β-cell function (52). We used the HOMA-B index, which reflects fasting β-cell function but cannot provide insight into the secretory response of β-cells to rising glucose concentrations. However, we are exploring to increase the number of time points during the OGTT.

Conclusion

Pancreatic iron is a powerful predictor for the alterations of glucose metabolism. Pancreatic iron is a strong predictor not only for cardiac iron but also for myocardial fibrosis and cardiac complications, supporting a more profound link between pancreatic iron and heart disease. If a patient has pancreatic iron overload, it would be prudent to intensify iron chelation therapy to prospectively prevent both alterations of glucose metabolism and cardiac iron accumulation rather than wait for overt diabetes and cardiac complications to appear, particularly in young patients. Preliminary studies have demonstrated that improvement in glucose metabolism is possible by combined DFP+DFO therapy (53), and we are waiting for prospective data from the E-MIOT project.

Acknowledgments. The authors thank all the colleagues involved in the E-MIOT project (https://emiot.ftgm.it/). The authors thank Claudia Santarlasci (Fondazione G. Monasterio CNR-Regione Toscana, Pisa, Italy) for her skillful secretarial work and all patients and the Italian Thalassaemia Foundation "L. Giambrone" for their cooperation.

Duality of Interest. A.Pep. is the principal investigator of the E-MIOT project, which receives "no-profit financial support" from industrial sponsorships (Chiesi Farmaceutici S.p.A., ApoPharma Inc., and Bayer). A.Pep., A.M., and L.P. received speakers' honoraria from Chiesi Farmaceutici S.p.A. No other potential conflicts of interest relevant to this article were reported.

The funders had no role in study design, data collection and analysis, or the decision to publish or in preparation of the manuscript.

Author Contributions. A.Pep. conceived and designed the study. L.P. was responsible for data collection. M.R.G., L.C., A.Pel., G.M., A.S., M.A., M.G.B., M.C.P., T.C., N.D.I., M.C., A.V., P.G., G.P., S.R., and R.R. collected the data. V.P. and V.D.S. assisted with the methods. A.M. performed the statistical analysis and drafted the initial manuscript. All authors assisted with interpretation, commented on drafts of the manuscript, and approved the final version. A.Pep. is the guarantor of this work and, as such, had full access to all the data in the study and takes responsibility for the integrity of the data and the accuracy of the data analysis.

Prior Presentation. Preliminary data of this study were presented at the following international congresses: 14th International Conference on Thalassemia and Haemoglobinopathies and 16th TIF International Conference for Patients and Parents, Thessaloniki, Greece, 17–19 November 2017; 59th American Society of Hematology Annual Meeting and Exposition, Atlanta, GA, 9–12 December 2017; Joint EuroCMR/SCMR Meeting, Barcelona, Spain, 31 January–3 February 2018; 23rd European Hematology Association Congress, Stockholm, Sweden, 14–17 June 2018; European Society of Cardiology Congress 2018, Munich, Germany, 25–29 August 2018; 24th European Hematology Association Congress, Amsterdam, the Netherlands, 13–16 June 2019; European Society of Cardiology Congress 2019 together with World Congress of Cardiology, Paris, France, 31 August–4 September 2019; and 61st American Society of Hematology Annual Meeting and Exposition, Orlando, FL, 7–10 December 2019.

References

1. Rund D, Rachmilewitz E. Beta-thalassemia. N Engl J Med 2005;353:1135–1146
2. Borgna-Pignatti C, Rugolotto S, De Stefano P, et al. Survival and complications in patients with thalassemia major treated with transfusion and deferoxamine. Haematologica 2004;89:1187–1193
3. Pepe A, Meloni A, Rossi G, et al. Cardiac complications and diabetes in thalassaemia major: a large historical multicentre study. Br J Haematol 2013;163:520–527
4. Chatterjee R, Bajoria R. New concept in natural history and management of diabetes mellitus in thalassemia major. Hemoglobin 2009; 33(Suppl. 1):S127–S130
5. Cario H, Holl RW, Debatin KM, Kohne E. Insulin sensitivity and beta-cell secretion in thalassaemia major with secondary haemochromatosis: assessment by oral glucose tolerance test. Eur J Pediatr 2003;162:139–146
6. Mavrogeni S, Pepe A, Lombardi M. Evaluation of myocardial iron overload using cardiovascular magnetic resonance imaging. Hellenic J Cardiol 2011;52:385–390
7. Maggio A, Capra M, Pepe A, et al. A critical review of non invasive procedures for the evaluation of body iron burden in thalassemia major patients. Pediatr Endocrinol Rev 2008;6(Suppl. 1):193–203
8. Noetzli LJ, Mittelman SD, Watanabe RM, Coates TD, Wood JC. Pancreatic iron and glucose dysregulation in thalassemia major. Am J Hematol 2012;87:155–160
9. Au WY, Lam WW, Chu W, et al. A T2* magnetic resonance imaging study of pancreatic iron overload in thalassemia major. Haematologica 2008; 93:116–119
10. Au WY, Lam WW, Chu WW, et al. A cross-sectional magnetic resonance imaging assessment of organ specific hemosiderosis in 180 thalassemia major patients in Hong Kong. Haematologica 2008;93:784–786
11. Meloni A, Restaino G, Missere M, et al. Pancreatic iron overload by T2* MRI in a large cohort of well treated thalassemia major patients: can it tell us heart iron distribution and function? Am J Hematol 2015;90:E189–E190
12. Noetzli LJ, Papudesi J, Coates TD, Wood JC. Pancreatic iron loading predicts cardiac iron loading in thalassemia major. Blood 2009;114: 4021–4026
13. Azarkeivan A, Hashemieh M, Shirkavand A, Sheibani K. Correlation between heart, liver and pancreas hemosiderosis measured by MRI T2* among thalassemia major patients from Iran. Arch Iran Med 2016;19:96–100
14. Pepe A, Positano V, Santarelli MF, et al. Multislice multiecho T2* cardiovascular magnetic resonance for detection of the heterogeneous distribution of myocardial iron overload. J Magn Reson Imaging 2006;23:662–668
15. Ramazzotti A, Pepe A, Positano V, et al. Multicenter validation of the magnetic resonance T2* technique for segmental and global quantification of myocardial iron. J Magn Reson Imaging 2009;30:62–68
16. Meloni A, De Marchi D, Pistoia L, et al. Multicenter validation of the magnetic resonance T2* technique for quantification of pancreatic iron. Eur Radiol 2019;29:2246–2252
17. Restaino G, Meloni A, Positano V, et al. Regional and global pancreatic T*2 MRI for iron overload assessment in a large cohort of healthy subjects: normal values and correlation with age and gender. Magn Reson Med 2011;65: 764–769
18. Positano V, Salani B, Pepe A, et al. Improved T2* assessment in liver iron overload by magnetic resonance imaging. Magn Reson Imaging 2009; 27:188–197
19. Meloni A, Positano V, Pepe A, et al. Preferential patterns of myocardial iron overload by multislice multiecho T*2 CMR in thalassemia major patients. Magn Reson Med 2010;64: 211–219
20. Positano V, Pepe A, Santarelli MF, et al. Standardized T2* map of normal human heart in vivo to correct T2* segmental artefacts. NMR Biomed 2007;20:578–590
21. Meloni A, De Marchi D, Positano V, et al. Accurate estimate of pancreatic T2* values: how to deal with fat infiltration. Abdom Imaging 2015; 40:3129–3136
22. Meloni A, Luciani A, Positano V, et al. Single region of interest versus multislice T2* MRI approach for the quantification of hepatic iron overload. J Magn Reson Imaging 2011;33:348–355
23. Wood JC, Enriquez C, Ghugre N, et al. MRI R2 and R2* mapping accurately estimates hepatic iron concentration in transfusion-dependent thalassemia and sickle cell disease patients. Blood 2005;106:1460–1465
24. Meloni A, Rienhoff HY Jr., Jones A, Pepe A, Lombardi M, Wood JC. The use of appropriate calibration curves corrects for systematic differences in liver R2* values measured using different software packages. Br J Haematol 2013;161:888–891
25. Meloni A, Maggio A, Positano V, et al. CMR for myocardial iron overload quantification: calibration curve from the MIOT Network. Eur Radiol 2020;30:3217–3225
26. Aquaro GD, Camastra G, Monti L, et al.; Working Group "Applicazioni della Risonanza Magnetica" of the Italian Society of Cardiology. Reference values of cardiac volumes, dimensions, and new functional parameters by MR: a multicenter, multivendor study. J Magn Reson Imaging 2017;45:1055–1067
27. Marsella M, Borgna-Pignatti C, Meloni A, et al. Cardiac iron and cardiac disease in males and females with transfusion-dependent thalassemia major: a T2* magnetic resonance imaging study. Haematologica 2011;96:515–520
28. Pepe A, Meloni A, Borsellino Z, et al. Myocardial fibrosis by late gadolinium enhancement cardiac magnetic resonance and hepatitis C virus infection in thalassemia major patients. J Cardiovasc Med (Hagerstown) 2015;16:689–695
29. Pepe A, Meloni A, Rossi G, et al. Prediction of cardiac complications for thalassemia major in the widespread cardiac magnetic resonance era: a prospective multicentre study by a multi-parametric approach. Eur Heart J Cardiovasc Imaging 2018;19:299–309
30. Pennell DJ, Udelson JE, Arai AE, et al.; American Heart Association Committee on Heart Failure and Transplantation of the Council on Clinical Cardiology and Council on Cardiovascular Radiology and Imaging. Cardiovascular function and treatment in β-thalassemia major: a consensus statement from the American Heart Association. Circulation 2013;128:281–308
31. Matthews DR, Hosker JP, Rudenski AS, Naylor BA, Treacher DF, Turner RC. Homeostasis model assessment: insulin resistance and beta-cell function from fasting plasma glucose and insulin concentrations in man. Diabetologia 1985;28:412–419
32. Wallace TM, Levy JC, Matthews DR. Use and abuse of HOMA modeling. Diabetes Care 2004; 27:1487–1495
33. De Sanctis V, Soliman AT, Elsedfy H, et al. The ICET-A recommendations for the diagnosis and management of disturbances of glucose homeostasis in thalassemia major patients. Mediterr J Hematol Infect Dis 2016;8:e2016058
34. Jessup M, Abraham WT, Casey DE, et al. 2009 focused update: ACCF/AHA guidelines for the diagnosis and management of heart failure in adults: a report of the American College of Cardiology Foundation/American Heart Association Task Force on Practice Guidelines: developed in collaboration with the International Society for Heart and Lung Transplantation. Circulation 2009;119:1977–2016
35. Buxton AE, Calkins H, Callans DJ, et al.; American College of Cardiology/American Heart Association Task Force on Clinical Data Standards (ACC/AHA/HRS Writing Committee to Develop Data Standards on Electrophysiology). ACC/AHA/HRS 2006 key data elements and definitions for electrophysiological studies and procedures: a report of the American College of Cardiology/American Heart Association Task Force on Clinical

Data Standards (ACC/AHA/HRS Writing Committee to Develop Data Standards on Electrophysiology). Circulation 2006;114:2534–2570
36. Cogliandro T, Derchi G, Mancuso L, et al.; Society for the Study of Thalassemia and Hemoglobinopathies (SoSTE). Guideline recommendations for heart complications in thalassemia major. J Cardiovasc Med (Hagerstown) 2008;9:515–525
37. De Sanctis V, Soliman AT, Elsedfy H, et al. Growth and endocrine disorders in thalassemia: the international network on endocrine complications in thalassemia (I-CET) position statement and guidelines. Indian J Endocrinol Metab 2013;17:8–18
38. Cappellini MD, Cohen A, Porter J, Taher A, Viprakasit V. *Guidelines for the Management of Transfusion Dependent Thalassaemia (TDT)*. 3rd ed. Nicosia, Cypress, Thalassaemia International Federation, 2014
39. Matter RM, Allam KE, Sadony AM. Gradient-echo magnetic resonance imaging study of pancreatic iron overload in young Egyptian beta-thalassemia major patients and effect of splenectomy. Diabetol Metab Syndr 2010;2:23
40. Brewer CJ, Coates TD, Wood JC. Spleen R2 and R2* in iron-overloaded patients with sickle cell disease and thalassemia major. J Magn Reson Imaging 2009;29:357–364
41. Cooksey RC, Jouihan HA, Ajioka RS, et al. Oxidative stress, beta-cell apoptosis, and decreased insulin secretory capacity in mouse models of hemochromatosis. Endocrinology 2004;145:5305–5312
42. Merkel PA, Simonson DC, Amiel SA, et al. Insulin resistance and hyperinsulinemia in patients with thalassemia major treated by hypertransfusion. N Engl J Med 1988;318:809–814
43. Angelopoulos NG, Zervas A, Livadas S, et al. Reduced insulin secretion in normoglycaemic patients with beta-thalassaemia major. Diabet Med 2006;23:1327–1331
44. Mowla A, Karimi M, Afrasiabi A, De Sanctis V. Prevalence of diabetes mellitus and impaired glucose tolerance in beta-thalassemia patients with and without hepatitis C virus infection. Pediatr Endocrinol Rev 2004;2(Suppl. 2):282–284
45. Zou DM, Sun WL. Relationship between hepatitis C virus infection and iron overload. Chin Med J (Engl) 2017;130:866–871
46. Kulaksiz H, Fein E, Redecker P, Stremmel W, Adler G, Cetin Y. Pancreatic beta-cells express hepcidin, an iron-uptake regulatory peptide. J Endocrinol 2008;197:241–249
47. Masini M, Campani D, Boggi U, et al. Hepatitis C virus infection and human pancreatic beta-cell dysfunction. Diabetes Care 2005;28:940–941
48. Midiri M, Lo Casto A, Sparacia G, et al. MR imaging of pancreatic changes in patients with transfusion-dependent beta-thalassemia major. AJR Am J Roentgenol 1999;173:187–192
49. Kosaryan M, Rahimi M, Darvishi-Khezri H, Gholizadeh N, Akbarzadeh R, Aliasgharian A. Correlation of pancreatic iron overload measured by T2*-weighted magnetic resonance imaging in diabetic patients with β-thalassemia major. Hemoglobin 2017;41:151–156
50. Omura T, Yoshiyama M, Hayashi T, et al. Core protein of hepatitis C virus induces cardiomyopathy. Circ Res 2005;96:148–150
51. Vassalle C, Petta S, Pepe A, Craxi A, Bondin M, Cacoub P. Expert opinion on managing chronic HCV in patients with cardiovascular disease. Antivir Ther 2018;23(Suppl. 2):35–46
52. Aono D, Oka R, Kometani M, et al. Insulin secretion and risk for future diabetes in subjects with a nonpositive insulinogenic index. J Diabetes Res 2018;2018:5107589
53. Farmaki K, Angelopoulos N, Anagnostopoulos G, Gotsis E, Rombopoulos G, Tolis G. Effect of enhanced iron chelation therapy on glucose metabolism in patients with beta-thalassaemia major. Br J Haematol 2006;134:438–444